LLNL-JRNL-421570

Analysis of micro-structural relaxation phenomena in laser-modified fused silica using confocal Raman microscopy

M. Matthews, R. Vignes, J. Cooke, S. Yang, J. Stolken

December 18, 2009

Optics Letters

Analysis of micro-structural relaxation phenomena in laser-modified fused silica using confocal Raman microscopy

Manyalibo J. Matthews*, Ryan M. Vignes, Juliet D. Cooke, Steven Yang and James S. Stolken

Lawrence Livermore National Laboratory,

7000 East Avenue, L-592, Livermore, CA 94550-9234 USA

Fused silica micro-structural changes associated with localized 10.6μm CO_2 laser heating are reported. Spatially-resolved shifts in the high-frequency asymmetric stretch transverse-optic (TO) phonon mode of SiO_2 were measured using confocal Raman microscopy, allowing construction of axial fictive temperature (T_f) maps for various laser heating conditions. A Fourier conduction-based finite element model was employed to compute on-axis temperature-time histories, and, in conjunction with a Tool-Narayanaswamy form for structural relaxation, used to fit $T_f(z)$ profiles to extract relaxation parameters. Good agreement between the calculated and measured T_f was found, yielding reasonable values for relaxation time and activation enthalpy in the laser-modified silica.

Keywords: structural relaxation; glass kinetics; fused silica; Raman microscopy; finite element analysis

**Corresponding Author – Present address: 7000 East Avenue, L-592, Livermore CA 94550, USA; 925-424-6762(ph); 925-422-5099(fax); email: ibo@llnl.gov*

Characterization of glass structure using vibrational spectroscopy has been used to study a wide range of glass-forming systems.[1-3] Glass *fictive* temperature, T_f, is defined as the temperature of the equilibrium melt whose structure is equivalent to that of the cooled glass, and has been a convenient tool in describing glass structural relaxation phenomena.[4] Technologically, changes in fictive temperature are known to affect mechanical, chemical and optical properties of heat-treated glasses, and are therefore important to assess in glass engineering. However, despite the numerous studies of structural relaxation in bulk-heated silica-based glasses, only recently[5-6] have studies attempted to address the application of standard relaxation models to fused silica glass treated with localized laser heating.

Geissberger and Galeener[1] first studied the changes in the SiO_2 Raman spectra as a function of T_f., establishing Raman spectroscopy as a useful tool for quantifying T_f. It was shown that open network silica Raman bands ω_i varied in frequency, while the 3- and 4-member ring 'defect' bands D_i varied in intensity, over the range $900 < T_f < 1700^oC$. For example, the Si-O-Si asymmetric stretch transverse-optic (TO) mode at ~1060 cm^{-1} was found to scale linearly with T_f as $\omega_{TO}(cm^{-1})=1082-17x10^{-3}T_f(^oC)$ and can be fit reasonably fit to a Gaussian. While the D_i bands can alternatively be used to characterize T_f, an additional benefit to measuring mode frequency shift is the ability to deduce the average Si-O-Si bond angle using central-force network dynamic models (CFNM),[7] thereby obtaining a measure of the thermally-induced densification caused by incomplete relaxation at high temperatures.

In this study we use confocal Raman microscopy to map volumetric structural changes in pristine SiO_2 induced by heating with a CO_2 laser. The dynamic temperature field during laser heating was determined by solving the nonlinear Fourier conduction heat equation using finite element modeling. A standard relaxation model is then used in conjunction with the calculated thermal histories to extract relaxation parameters from the measured Raman data as a function of depth. The non-uniform fictive temperature profiles were found to be well described by our analysis, showing for the first time to our knowledge, the direct application of the Tool-Narayanaswamy relaxation model in describing laser-heated silica.

A polished UV-grade Corning 7980 fused silica sample was used in the present study, 10mm thick by 51mm diameter round. 10.6 μm continuous-wave (CW) light from a Synrad firestar V20 CO_2 laser was focused to a 1.0±0.1mm $1/e^2$ diameter spot at the sample surface. Beam power, diameter and surface temperature were all monitored in real time using methods described elsewhere.[8] Following a 10 s hold, laser power was linearly ramped down over 1, 3, 10, 30 and 100 s using an acousto-optic modulator until the peak temperature was ~1400K, and then quenched. This resulted in power (temperature) ramp rates of approximately 2.0 (68), 0.67 (23), 0.20 (6.8), 0.067 (2.3) and 0.020 (0.68) W/s (K/s) respectively. Relative sample position was controlled using an active-feedback piezoelectric stage with a positioning accuracy better than 10 nm. Raman scattering measurements were carried out using a diode-pumped frequency-doubled Nd-YVO_4 CW laser operating at 532 nm in a back-scattering collection geometry. A 100x/0.70NA objective lens was used as the focus and collection optic. Back-scattered light was filtered through a 532nm notch filter before being focused into a 50 μm core multimode fiber/pinhole using a 5x/0.14NA objective. The axial and lateral spatial resolution was ~4 μm and ~2 μm respectively, in good agreement with predictions for a pinhole-limited confocal system.[9] Filtered Raman light was dispersed through a Ne lamp-calibrated f/4 spectrophotometer equipped with a 1200 gr/mm, 500 nm-blazed holographic grating and a LN-cooled 1100x300 pixel back-illuminated CCD, yielding a spectral resolution and accuracy of ~4 cm^{-1} and <1 cm^{-1}, respectively. The total integration time for each spectrum was 30 s.

Figure 1 exemplifies the range of measured TO-phonon frequency (ω_{TO}) shifts, and the computed $T_f(z)$ values using Ref. 1 (symbols) for two of the cases studied, namely a power ramp of 0.7W/s over 30 s and 2W/s over 1 s. ω_{TO} was determined from each spectra through a least-squares Gaussian fit of the TO-mode peak. Beyond ~150 μm, ω_{TO} was unchanged from the as-received value of ~1060 cm^{-1} for all cases studied, while near the surface and peak treatment temperature region ω_{TO} varied from 1052~1056 cm^{-1}, depending on treatment. These lower frequency values corresponded to thermally-induced Si-O-Si bond angle shifts[10] of *-2* ~ -3 degrees and densifications of 1~2%. Similar to the results of Zhao *et al.* for short pulse CO_2 exposures[6], $T_f(z)$ was found to follow a sigmoidal curve, decreasing into the bulk to initial T_f values close to T_g. The depth of the heat-affected region characterized by T_f scaled with the exposure time, as longer times allowed deeper regions with longer relaxation times to achieve thermodynamic equilibrium. Similarly, the slower temperature ramps also allowed surface regions to more fully relax, resulting in a lower surface fictive temperature relative to the faster ramped cases.

Below the evaporation threshold of SiO_2 (~2500 K), it has been shown[8] that CO_2 laser heat transport can be well-approximated by considering phonon conduction only, and can be described through finite element analysis of the nonlinear (Fourier) heat diffusion equation,

$$\rho C_p \frac{\partial T}{\partial t} = \nabla \cdot (k \nabla T) + Q \qquad (1)$$

where ρ, C_p and k are the density, specific heat capacity under constant pressure and the thermal conductivity respectively. In Eq. 1, Q is the time-dependent volumetric laser heating source specified in cylindrical coordinates as $Q(r,z,t) = \alpha(T)I(t)e^{-\alpha(T)z}e^{-2r^2/w^2}$ for an absorption length α, irradiance I and $1/e$ beam radius w. We use data from McLachlan[11] and Wray[12] for the temperature dependence of α and k respectively, while C_p is approximated by analytic expressions from Smyth.[13] ρ varies less than 1% over 300-2000 K[14] and is taken as constant, ρ=2.2 g/cm^3. The energy deposition was sufficiently resolved within the absorption depth of the surface (α^{-1}~4 μm at 2000 K) by using a highly non-uniform mesh of 22,000 elements ranging from 2x2 μm meshing directly below the laser and 30x30 μm meshing at the bottom outside edge of the sample. $T(r,z,t)$ was computed over ~2100 time steps and, for comparison with the Raman data, extracted along r=0 at 152 axial positions.

Phenomenologically, the fictive temperature can be described in terms of the local thermal history $T(r,z,t)$ and a relaxation function $M(T, T_f, \tau)$ specific to the glass system in question,[15-17]

$$T_f = T - \int_0^t M(T, T_f, \tau) \frac{\partial T}{\partial t'} dt' \tag{2}$$

where τ is the structural relaxation time. The exact form of $M(T, T_f, \tau)$, is a subject of continued debate and refinement, but can reasonably described[17] by $M=exp(-t/\tau)^\beta$ where the Kohlrausch exponent β ranges over 0.7~1 for fused silica. However, for simplicity, we approximate β=1 and use a single relaxation time given by[15]

$$\tau(T, T_f) = \tau_0 \exp\left[\left(\frac{\Delta h}{R}\right)\left(\frac{x}{T} + \frac{1-x}{T_f}\right)\right] \tag{3}$$

which is expressed in terms of an activation enthalpy Δh, relaxation time constant τ_0, and a structure factor $0<x<1$ specifying the relative contributions of the instantaneous and integrated thermal histories. Eqs. (3), known as the Tool-Narayanaswamy relaxation time, has been found to most reasonably describe bulk-heated glass relaxation for a wide variety of a glass forming systems.[4] The measured $T_f(z)$ data can now be fit by inserting the calculated $T(z,t)$ axial temperature histories from Eq.(1) into Eq.(2), and allowing x, Δh and τ_0 to vary as fit parameters. For each fit/calculation the initial fictive temperature was set to the manufacturer's reported annealing temperature, $T_f(0)$ =1315 K, which was, in fact, within the sampling error bars of our T_f measurements of unexposed sample regions (T_f = 1307±13 K).

Shown in Fig. 1 along with the measured Raman data are fits to $T_f(z)$ obtained using Eq. (2), from which τ_0, Δh and x were extracted for all cases studied. For convenience, the relaxation time τ_R at T = 1315 K ($\approx T_g$) was computed, and along with Δh and x is shown for each of the ramp cases in Fig. 2. An activation energy of ~250kcal/mole was found for all cases, consistent with small X-ray scattering experiments[18] of bulk-heated type-III silica in which the Adam-Gibbs parameter Q_{AG}=39±9x10^3 K can be equated to values of Δh~320±70 kcal/mole.

However, both x and τ_R varied monotonically with exposure parameters, both increasing with decreasing ramp rate and longer exposure. Except for the longest ramp case (0.007 W/s, 100 s), the range of values found for the structure parameter x, 0.25~0.79 were relatively close to the values typically found for silicates (0.4~0.6).[4] Larger values of x could indicate a decreasing importance of structural history, though x is generally expected to constant for a given glass structure. At short ramp times (2 to 0.2 W/s) the relaxation time at 1315 K ranged from ~60 to ~300 s, close to the shear stress relaxation time $\tau_s=\eta(1315\ K)/G_\infty$=127 s, as estimated from viscosity (η) data for type-III silica[19] and a high frequency shear modulus G_∞~31GPa. While the variation in relaxation time (and structure factor) could be a result of our over-simplified rheological construction (β=1), an alternative consideration is that the configurational or content changes in hydroxyl groups may influence relaxation near the laser irradiated surface.[20]

We have reported on the spatially-resolved fictive temperature measurements of laser-modified fused silica. After establishing thermal history maps using finite element analysis, a simplified Tool-Narayanaswamy relaxation model with a single relaxation time was found to reasonably describe the spatial dependence of T_f for different cooling rates. The resulting relaxation parameters were in general agreement with previously found values for type-III silica, though changes in the structure factor and relaxation time are not yet completely understood. Future work will seek to clarify the possible role of diffusing species such as OH groups, and study the effect of β<1 in our model.

This work performed under the auspices of the U.S. Department of Energy by Lawrence Livermore National Laboratory under Contract DE-AC52-07NA27344.

1. A. E. Geissberger and F. L. Galeener, Phys. Rev. B **28** (6), 3266-3271 (1983).
2. S. R. Ryu and M. Tomozawa, J Non-Cryst Solids **352** (36-37), 3929-3935 (2006).
3. B. Kuhn and R. Schadrack, J Non-Cryst Solids **355** (4-5), 323-326 (2009).
4. G. W. Scherer, J Non-Cryst Solids **123** (1-3), 75-89 (1990).
5. T. D. Bennett and L. Li, J. Appl. Phys. **89** (2), 942-950 (2001).
6. J. Zhao, J. Sullivan, J. Zayac and T. D. Bennett, J. Appl. Phys. **95** (10), 5475-5482 (2004).
7. F. L. Galeener, J Non-Cryst Solids **49** (1-3), 53-62 (1982).
8. S. T. Yang, M. J. Matthews and S. Elhadj, J. Appl. Phys. **106** (10), 1031061-1031067 (2009).
9. T. R. C. a. G. S. Kino, *Confocal Scanning Optical Microscopy and Related Imaging Systems*. (Academic Press, San Diego, 1996).
10. F. L. Galeener, Solid State Commun **44** (7), 1037-1040 (1982).

11. A. D. McLachlan and F. P. Meyer, Appl Optics **26** (9), 1728-1731 (1987).
12. K. L. Wray and T. J. Connolly, J. Appl. Phys. **30** (11), 1702-1705 (1959).
13. H. T. Smyth, H. S. Skogen and W. B. Harsell, J Am Ceram Soc **36** (10), 327-328 (1953).
14. R. Bruckner, J Non-Cryst Solids **5**, 123-175 (1970).
15. O. S. Narayanaswamy, J Am Ceram Soc **54** (10), 491-& (1971).
16. C. A. Angell, Science **267** (5206), 1924-1935 (1995).
17. O. Alejos, C. deFrancisco, P. Hernandez, K. Bendimya and J. M. Munoz, Appl. Phys. A-Mater. Sci. Process. **63** (5), 471-474 (1996).
18. R. Bruning, C. Levelut, A. Faivre, R. LeParc, J. P. Simon, F. Bley and J. L. Hazemann, Europhys Lett **70** (2), 211-217 (2005).
19. V. Zandian, J. S. Florry and D. Taylor, Brit Ceram Trans J **90** (2), 59-60 (1991).
20. N. Shen, M. J. Matthews, J. E. Fair, J. A. Britten, H. T. Nguyen, D. Cooke, S. Elhadj and S. T. Yang, Applied Surface Science (submitted) (2009).

FIGURE CAPTIONS

Figure 1: Measured Si-O-Si asymmetric stretch TO mode frequency shift and fictive temperature as a function of depth for 2W/s and 0.7W/s laser power ramps (symbols) each fit to the relaxation model cited in the text (lines). Experimental error bars are derived from the 95% confidence interval data of the reference. [1] The dashed line indicates the glass manufacturer's quoted annealing (glass transition) temperature.

Figure 2: Activation enthalpy, relaxation time at 1315 K and structure factor derived from fits to Eq. 2 as a function of laser power ramp rate. Error bars shown correspond to the 95% confidence interval of the least-squares fitting.

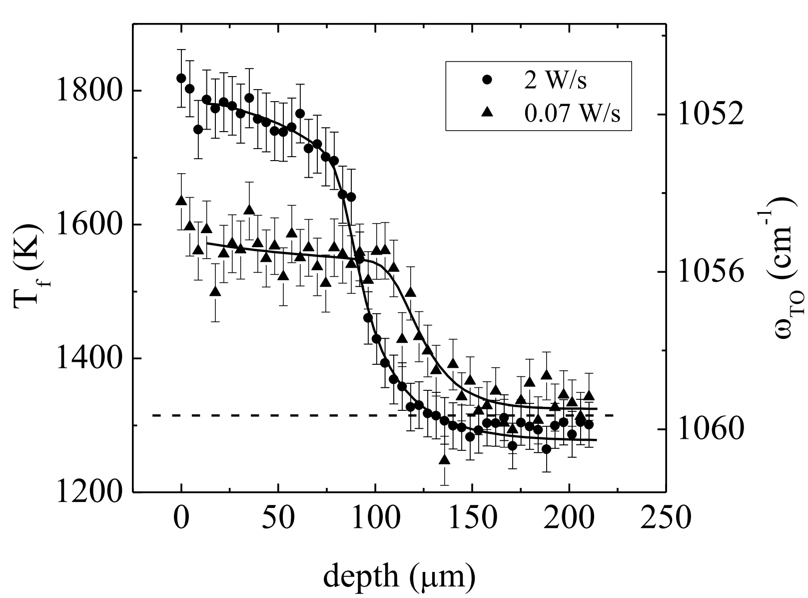

FIGURE 1

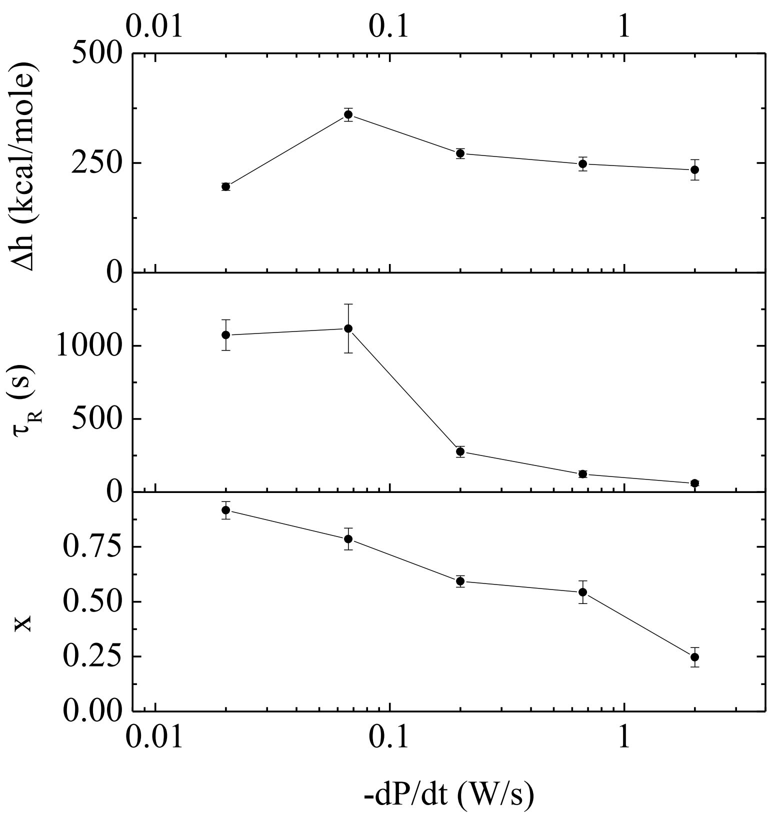

FIGURE 2